A heat transfer study for beamline components in high-power wiggler and undulator beamlines. Part I. Beam stops (invited)

M. J. Bedzyk

Cornell High Energy Synchrotron Source (CHESS), and the School of Applied and Engineering Physics, Cornell University, Ithaca, New York 14853

M. J. Keeffe

Cornell High Energy Synchrotron Source (CHESS), Cornell University, Ithaca, New York 14853

W. Schildkamp

Section of Biochemistry, Molecular, and Cell Biology, and Cornell High Energy Synchrotron Source (CHESS), Cornell University, Ithaca, New York 14853

Q. Shen

The School of Applied and Engineering Physics, Cornell University, Ithaca, New York 14853

(Presented on 30 August 1988)

The heat transfer capabilities of beam stops in CHESS wiggler and undulator beamlines is described. The thermal analysis for the design of these crucial in-vacuum beamline components is based on the use of a finite element analysis computer calculation and experimental heat loading tests.

The integrity of a high-power insertion device beamline is crucially dependent on the capability of cooling in-vacuum components that must be able to absorb all, or a significant fraction, of the total synchrotron radiation power. In Part I of this article, we will describe the heat transfer capability of the existing water-cooled beam stops (x-ray shutters) at the Cornell High Energy Synchrotron Source (CHESS). These components have withstood a maximum total power output of 5 kW from a 6-pole electromagnet (EM) wiggler and 1 kW from a 123-pole permanent magnet (PM) undulator. We will also discuss a newly designed beam stop that will be installed in a new beamline at CHESS which will receive up to 14 kW of radiative power from a 24-pole PM wiggler. In Part II of this report[1] a thermal stress analysis for the beryllium filters and Be windows used in these beamlines will be given.

The parameters used for characterizing the angular power distribution from each of these insertion devices is given in Table I. The expressions, which use the ring energy E_R and current I_R, number of periods N, period length λ_u, and peak magnetic field B_0, for calculating the deflection parameter K, on axis critical energy E_c, maximum horizontal deflection angle δ, on axis radiated power per unit solid angle $dP_0/d\Omega$, on axis power per unit horizontal angle $dP_0/d\theta$, and total power P_T can be found in Refs. 2 and 3. Note that the zero emittance values for power density listed in Table I are proportional to E_R raised to the fourth power. While this $dP_0/d\Omega \propto E_R^4$ feature is a principle motivation for using high-energy storage rings as synchrotron radiation sources, it also presents certain special demands for cooling designs of beamline components. In this respect, the one saving feature of a higher energy E_R is that the inherently higher critical energy of the power spectrum distributes the power more deeply into an absorber.

The water-cooled copper beam stop in the CHESS A-line that has been used as a shutter for both the EM wiggler and the PM undulator is depicted in Fig. 1. Using the PHOTON program[4] with the Table I parameters for $E_R = 6$ GeV, we calculate that 49% of the wiggler power and 87% of the undulator power is absorbed and converted into heat in the first 0.1 mm of the 7-mm-thick front Cu face. Similarly, 82% of the EM wiggler power and 99% of the undulator power is absorbed in the first 1 mm.

This absorbing Cu slab, which is perpendicular to the incident beam direction, is followed by a 6.4-mm-thick channel containing 30 °C water for cooling by forced convection. The 3 gal/min (11.4 ℓ/min) turbulent flow combined with the channel dimensions results in a film coefficient of $h_f = 1.2$ W/°C/cm^2 at the bulk temperature $T_b = 30$ °C. This h_f value, which has been experimentally verified in a separate study, will be assumed to be constant with temperature. This is a conservative approximation as long as the film temperature T_f at the Cu/water interface stays below boil-

TABLE I. CHESS insertion device power and power density characteristics for $E_R = 5$–6 GeV and $I_R = 100$ mA.

	EM wiggler	PM wiggler	PM undulator
N	3	12	61
λ_u (cm)	34.3	19.6	3.3
$B_0(T)$	1.5	1.24	0.5
K	48.1	22.6	1.54
E_c (keV)	24.9–35.9	20.6–29.6	8.33–12.0
δ (mrad)	4.92–4.10	2.30–1.92	0.157–0.131
$dP_{0/d\Omega}$ (kW/mrad^2)	3.05–6.32	10.1–20.9	20.1–41.7
$dP_{0/d\theta}$ (kW/mrad)	0.475–0.820	1.57–2.72	2.23–5.59
P_T (kW)	3.67–5.28	5.69–8.19	0.799–1.15

 0034-6748/89/071460-04$01.30

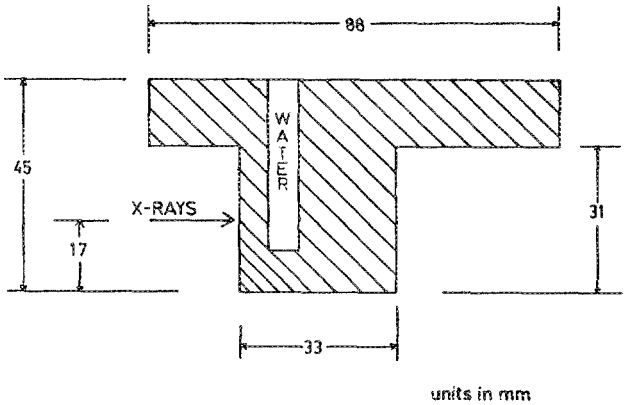

FIG. 1. Cross-sectional side view of the existing CHESS copper beam stop.

ing, which is $T_{sat} = 144$ °C at the channel water pressure of 60 psia (4.1 atm).

The Cu is characterized in these calculations by a temperature dependent thermal conductivity k that is 3.99 W/cm/°C at 30 °C and drops off in roughly a linear fashion to 3.34 W/cm/°C at 1000 °C. The melting temperature of Cu is 1083 °C.

The temperature profiles shown in Fig. 2 for this Cu beam stop were calculated using ANSYS—a finite element engineering program,[5] with three dimensional isoparametric (STIF 70) thermal solid elements. (Two dimensional analysis drastically overestimated the temperatures when the horizontal width of the beam is significantly shorter than the water channel width.) Due to symmetry, the analysis is reduced to solving for the temperature in one quadrant of the beam stop. After dividing the solid model shown in Fig. 2 into ~1400 elements of appropriate sizes, elements in the beam path were assigned heat densities (W/mm^3) based on the power absorbed output of the PHOTON program and the

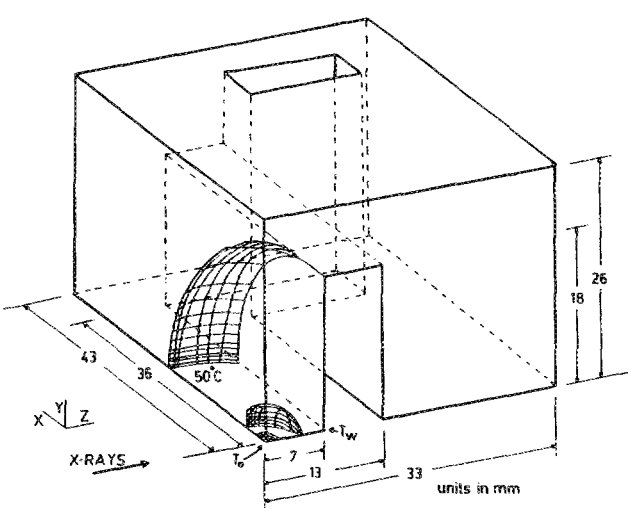

FIG. 2. Computed temperature distribution for the one-fourth beam stop model used in the thermal analysis of existing CHESS beam stop shown in Fig. 1. The heat load distribution for the 123-pole PM undulator at 6 GeV and 100 mA was used for this calculation. See Tables I, III, and V. The outer most temperature contour is at 50 °C, the next is at 150 °C, and the inner most is at 250 °C.

TABLE II. Zero emittance beam size and total power per unit area at the beam stop distance L_{bs}. $E_R = 5$–6 GeV and $I_R = 100$ mA.

	EM wiggler	PM wiggler	PM undulator
L_{bs} (m)	8.2	9.7	12.2
$\Delta\theta$ (mrad)	7.73–6.44	3.62–3.02	0.247–0.206
ΔX (mm)	63.4–52.8	35.2–29.3	3.01–2.51
ΔY (mm)	1.27–1.06	1.50–1.25	1.88–1.57
dP/dA (W/mm^2)	45.3–94.0	107.0–222.0	135.0–280.0

beam size. The beam width ΔX, height ΔY, and total power per unit area dP/dA for the beam stop distance L_{bs} from the sources is given in Tables II–IV. These values are based on rectangular distribution approximation[2] for $dP/d\Omega$ that has a full width horizontal opening angle of $\Delta\theta = (\pi/2)\delta$ and vertical opening angle $\Delta\psi = 1.52/\gamma$. ($\Delta\psi = 0.155$ mrad at 5 GeV and 0.129 mrad at 6 GeV).

$$\Delta X = 2\{\sigma_x^2 + [\sigma_{x'}^2 + (\Delta\theta/2)^2]L^2\}^{1/2}, \quad (1)$$

$$\Delta Y = 2\{\sigma_y^2 + [\sigma_{y'}^2 + (\Delta\psi/2)^2]L^2\}^{1/2}. \quad (2)$$

Table II gives the zero emittance values (i.e., $\sigma_i = \sigma_f = 0$) for the beam size and power per unit area. Table III gives the corresponding values that the Cornell Electron Storage Ring (CESR) was operated in during the low emittance spring 1988 undulator run,[6] while Table IV gives the corresponding values when CESR operates for High Energy Physics (HEP).

For comparison, the power density at the anode of a 1 kW x-ray tube is ~100 W/mm^2. The CHESS exit port crotches[7] are rated for a power density of 800 W/mm^2. This is the power density from the hard bend dipole magnet at a 2 m distance if CESR were operating at 8 GeV and 100 mA.

To be conservative, we will insist that the beam stop must satisfy design criteria for the power density at the low emittance condition described in Table III. Design criteria are: (1) all points in the beam stop should stay at least 200° below melting and (2) no point in the turbulent layer at the Cu/water interface exceed the boiling point. We will assume that the turbulent layer film temperature T_f is the average between the Cu wall T_w and the bulk water temperature T_b. Therefore, the Cu temperature at the Cu/water interface T_w should not exceed 258 °C for 30 °C water at 60 psia. To check the beam stop designs, we ran the ANSYS calculation and noted this T_w temperature and the maximum temperature T_0 at the beam center of the front surface. Table V lists the

TABLE III. Low emittance beam size and power per unit area at the beam stop $\sigma_x = 1.14$ mm, $\sigma_{x'} = 0.057$ mrad, $\sigma_y = 0.059$ mm, $\sigma_{y'} = 0.012$ mrad. $E_R = 5$–6 GeV and $I_R = 100$ mA.

	EM wiggler	PM wiggler	PM undulator
ΔX (mm)	63.4–52.8	35.2–29.4	4.03–3.67
ΔY (mm)	1.29–1.08	1.53–1.28	1.92–1.61
dP/dA (W/mm^2)	44.9–92.6	106.–218	103.–195.

TABLE IV. HEP emittance beam size and power per unit area at the beam stop $\sigma_x = 1.3$ mm, $\sigma_{x'} = 0.15$ mrad, $\sigma_y = 0.4$ mm, $\sigma_{y'} = 0.05$ mrad. $E_R = 5$–6 GeV and $I_R = 100$ mA.

	EM wiggler	PM wiggler	PM undulator
ΔX (mm)	63.5–52.9	35.3–29.6	5.41–5.15
ΔY (mm)	1.71–1.56	1.96–1.77	2.39–2.15
dP/dA (W/mm^2)	33.8–64.0	82.2–156.	61.8–104.

outcome of the calculations for the modeled beam stop shown in Fig. 2 in terms of these two temperatures.

Table V values indicate that this beam stop design satisfies the criteria for the 6-pole EM wiggler and 123-pole PM undulator at 6 GeV and 100 mA. This beam stop has in fact operated successfully under conditions equivalent to these. However, this beam stop design is clearly unsatisfactory for operation with the proposed 24-pole PM wiggler at 6 GeV and 100 mA.

By comparing the EM wiggler results to the PM undulator results given in Table V, we can easily see that the temperature at the water surface T_w is strongly affected by the total power, while the temperature at the front hot spot T_0 is most strongly affected by the power density.

A concluding statement for this beam stop is that the thermal analysis predicts that it will be able to operate up to 200 ma at 5 GeV for both the 6-pole EM wiggler and 123-pole PM undulator.

To satisfy the beam stop design criteria for the 24-pole PM wiggler, we have designed and built a Be/Cu 15°-wedge shaped beam stop to go into this new beamline. (See Fig. 3.) The front hot spot temperature T_0 for this design is lower since the 15° incident angle reduces the effective surface power density by a factor of 4 and since 1 mm of beryllium only absorbs 10% of the total power. (This same length of Cu would absorb 86% of the total power from the PM wiggler at 6 GeV.) Since there is more material between the hot spot and the water channel, and since Be has a longer x-ray absorption length than Cu, this design also allows the heat to diffuse outward more uniformly from the hot spot, and thus reduces the maximum temperature T_w a the Cu water interface in comparison to the previous design. By making the shape of the water-cooling channel serpentine, we have increased the cooling surface area and increased the heat transfer coefficient to $h_f = 1.7$ W/cm^2/°C for 4.5 gal/min water at $T_b = 30$ °C. Similar Be heat diffusers have been in operation for eight years as part of the CHESS exit ports (crotches)[7].

TABLE V. Cu temperatures for the beam stop shown in Fig. 2 and for power distribution described by Table III. $E_R = 5$–6 GeV and $I_R = 100$ mA.

	EM wiggler	PM wiggler	PM undulator
T_0 (°C)	287–458	712–> 1083	445–701
T_w (°C)	151–233	317–400	94–124

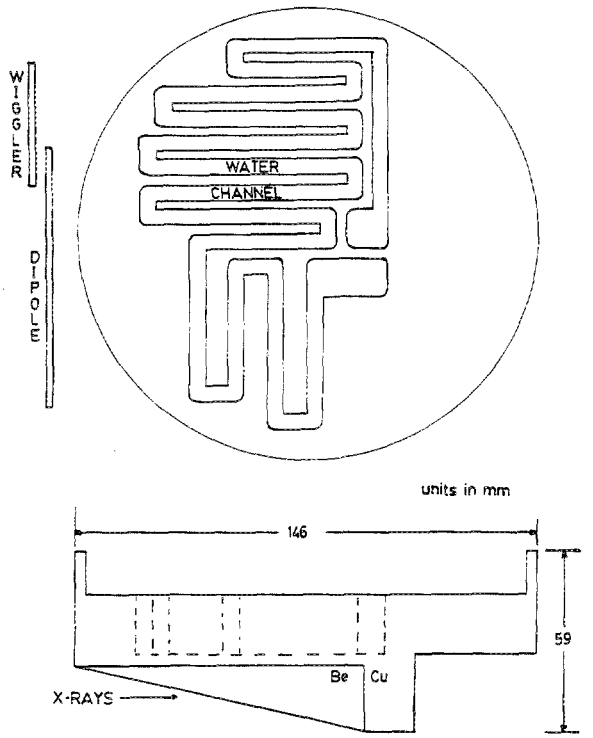

FIG. 3. Top and side view of Be/Cu 15° wedge-shaped beam stop. The top view also shows the relative positions of beams from the 24-pole PM wiggler and hard-bend dipole magnet. The wiggler power density is ~50 times greater than the dipole power density.

A side-view sectional plot from the 3D ANSYS calculation for the model of this beam stop is shown in Fig. 4. Table VI lists the maximum temperatures at the Be front surface T_0, the Be/Cu brazed interface T_1, and the Cu/water interface T_w. While relative temperatures $(T_w - T_b)$ and $(T_1 - T_b)$ double when the current is doubled at 5 GeV, the $(T_0 - T_b)$ relative temperature increases by a factor of 2.4 for a current change from 100 mA to 200 mA at 5 GeV. This nonlinearity is due to the significant drop off in the Be thermal conductivity at these elevated temperatures. For Be

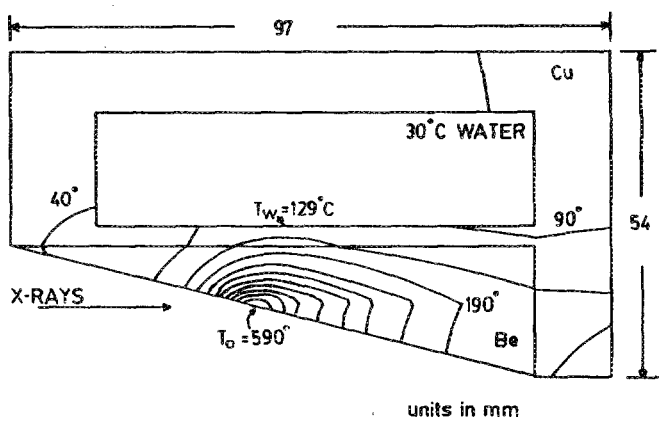

FIG. 4. Computed temperature distribution for the beam stop model used in the thermal analysis of Be/Cu wedge-shaped beam stop shown in Fig. 3. The heat load distribution for the 24-pole PM wiggler at 6 GeV and 100 mA was used in this calculation. See Tables I, III, and VI. Temperature contours are in 50 °C increments starting at 40 °C.

TABLE VI. Calculated temperatures in the Be/Cu wedge beam stop shown in Fig. 4 for the PM wiggler power distribution described in Table III.

E_R (GeV)	I_R (mA)	T_0 (°C)	T_1 (°C)	T_w (°C)
5	100	363	105	93
6	100	590	148	129
5	200	837	183	158

$k = 2.0$ W/cm/°C at 30 °C, 1.0 W/cm/°C at 700 °C, and 0.9 W/cm/°C at 1000 °C. The melting temperature of Be is 1278 °C.

ANSYS thermal analysis calculations have also been made for the beam stop shown in Fig. 1, but with a 5-mm-thick Be slab added to the front face. When heated by the 24-pole PM wiggler at 6 GeV and 1000 mA, this design predicts Cu temperatures at the water surface far in excess of the $T_w = 258$ °C criteria. For an all-Cu-15°-wedge-shaped beam stop design similar to Figs. 3 and 4 (but, without Be), and heated by the PM wiggler power at 6 GeV and 100 mA, the front hot spot was $T_0 = 670$ °C and $T_w = 190$ °C. While possibly acceptable at this power level, this all-copper wedge design would not be able to withstand the power load from the PM wiggler when CESR reaches an anticipated current of 200 mA during 14 bunch operation. The Be/Cu wedge beam stop, on the other hand, with a Be heat diffuser insert will be able to operate up to 200 mA at 5.5 GeV.

Another design that will withstand these extreme power density conditions is the 6° Cu wedge thermal absorber[8] used in the new x-ray wiggler beamlines at the National Synchrotron Light Source at Brookhaven National Laboratory. We found, however, that such a small angle of inclination required a beam stop length which exceeded our design criteria.

In conclusion, the thermal design principles developed for this 15° Be/Cu wedge shaped beam stop should be applicable for insertion device beamlines in the soon to be built high energy dedicated storage ring facilities, since the total power output and peak power densities from the CHESS insertion devices will approach the design values for the new facilities.

[1]Q. Shen, M. J. Bedzyk, M. J. Keeffe, and W. Schildkamp (see following article this issue).
[2]K.-J. Kim, Nucl. Instrum. Methods A **246**, 67 (1986).
[3]H. Winick, in *Synchrotron Radiation Research*, edited by H. Winick and S. Doniach (Plenum, New York, 1979), p. 11.
[4]D. Chapman, N. Gmur, N. Lazarz, and W. Thomlinson, Nucl. Instrum. Methods A **266**, 191 (1988).
[5]ANSYS. Engineering Analysis Systems, Swanson Analysis Systems Inc., Houston, PA 15342.
[6]D. H. Bilderback, B. W. Batterman, M. J. Bedzyk, K. Finkelstein, C. Henderson, A. Merlini, W. Schildkamp, Q. Shen, J. White, E. B. Blum, P. J. Viccaro, D. M. Mills, S. Kim, G. K. Shenoy, K. E. Robinson, F. E. James, and J. M. Slater (these proceedings).
[7]D. M. Mills, D. H. Bilderback, and B. W. Batterman, IEEE Trans. Nucl. Sci. **NS-26**, 3854 (1979).
[8]S. Ulc and S. Sharma, Nucl. Instrum. Methods A **246**, 423 (1986).